

Lithium-sulfur batteries

Linda F. Nazar, Marine Cuisinier, and Quan Pang

Markets for energy storage that go beyond portable electronics have emerged rapidly this decade, including powering electric vehicles and "leveling the grid" fed by renewable sources such as solar energy, which are intermittent in supply. These new demands require a significant step-up in energy density that will probably not be met by Li-ion batteries; estimates suggest they are starting to approach their theoretical limits. But in the world of "beyond Li-ion," the options are limited. One of the most hopeful is the Li-S battery, for which greater energy storage can potentially be realized through phase-transformation chemistry using elemental sulfur as a positive electrode material, which converts to lithium sulfide. These future generation systems offer up to a five-fold increased specific energy and greatly reduced cost factors, but commercialization has been hindered owing to key challenges. Efforts over the last two years to better manipulate the cell chemistry and overcome these challenges are presented.

Introduction

Today's world has been unalterably changed by rechargeable lithium-ion (Li-ion) batteries that power a multitude of indispensable portable electronic devices owing to their relatively high energy density. This was recognized this year with the award of the Draper Prize for Engineering to the founders of the technology.[1] These batteries have found their way into the hybrid and electric vehicle market with ever-increasing popularity and are also gradually starting to make inroads into larger-scale energy storage for renewable energy sources such as solar power. Over 200 MWs of Li-ion batteries are installed globally for grid applications at present,[2] and this number is predicted to increase as the need to manage the intermittency of renewable generation rises. At the same time, the inherent limitations of Li-ion batteries based on Li^+ insertion/extraction chemistry are becoming apparent, which include both cost and performance factors.[3,4]

Although much effort is being expended to create next-generation Li-ion systems, it is also appreciated that they are approaching their energy density boundaries, anticipated to have a ceiling about double that of today's cells. Their price remains an impediment to achieving the 3–5-fold decrease in cost regarded as necessary for widespread penetration of electric vehicles in the automotive market, with even lower cost per kWh being essential for grid storage. New directions are needed to inspire change for energy storage systems that differ from conventional Li-ion systems.

Lithium-sulfur (Li-S) batteries provide a promising option that could theoretically achieve the necessary step up, considering both cost and specific energy. Elemental sulfur—abundant and inexpensive—has become one of the most actively researched cathode materials in the last few years, with 445 papers published since 2012 alone at the time of writing. Its high theoretical specific capacity is based on a redox reaction that reversibly interconverts sulfur and Li_2S via intermediate lithium polysulfide species (Li_2S_n, $n = 2–8$).[5,6] The chemistry is fundamentally different from the intercalation process that governs Li-ion cells and has higher energy density, but it comes with several challenges. Li-S cells have suffered from low sulfur utilization and poor long-term cycling in the past; they experience a large volumetric expansion upon formation of Li_2S; and the dissolution of lithium polysulfide intermediate species in commonly used liquid electrolytes triggers a parasitic shuttle-type diffusion process of Li_2S_n polysulfides that can result in low Coulombic efficiency.[7] Although many significant achievements have been made recently to overcome these shortcomings, additional inroads in materials and understanding of the dissolution-precipitation cell chemistry are still required in order to realize the promise of the technology. Because several recent excellent reviews are available

Linda F. Nazar, University of Waterloo, Ontario, Canada; lfnazar@uwaterloo.ca
Marine Cuisinier, University of Waterloo, Ontario, Canada
Quan Pang, University of Waterloo, Ontario, Canada
DOI: 10.1557/mrs.2014.86

© 2014 Materials Research Society
https://doi.org/10.1557/mrs.2014.86 Published online by Cambridge University Press

on Li-S,[3,8–12] this article is not intended to be all-inclusive, but rather it is intended to provide an overview.

Energy storage basics

Energy density is the product of the cell voltage (V) and the specific capacity (A h g^{-1} or A h L^{-1}) based on the total mass/volume of the positive ("cathode") and negative ("anode") electrodes. In a Li-ion battery, Li^+ ions shuttle between the positive electrode intercalation host, where they are stored upon discharge (i.e., a layered oxide $LiMO_2$ where M is composed of Co, Ni, Mn, and Al; or a phosphate such as $LiFePO_4$), and the graphitic carbon negative electrode, where they are stored on charging to a maximum content of $Li_{0.16}C$. The inherent atomic structure of both the negative and positive electrode host materials is maintained throughout cycling. Cell voltages are in the range of 3.4–3.8 V (versus Li), with theoretical capacities at the positive electrode as high as 280 A h g^{-1}. Theoretical energy densities are around 390 Wh kg^{-1} for a full cell, which contains all components, but practical values approach 210 Wh kg^{-1} and much less than that for "battery packs."

The Li-S cell is quite different. The positive electrode consists of a porous, electronically conducting host, a vital component that delivers electrons to the insulating sulfur. Upon discharge, the Li^+ ions oxidized from the lithium negative electrode migrate through the electrolyte to join up with the electrons passed via the external circuit. The sulfur is reduced to Li_2S, which is also an excellent insulator. The reaction is surprisingly reversible. The theoretical energy density is determined by the overall cell reaction, $S_8 + 16Li \leftrightarrow 8Li_2S$ and its potential of 2.15 V versus Li/Li^+. Although the voltage is lower than for commercial intercalation materials, it is compensated by the specific capacity that is the highest of any solid electrode material at 1,675 mA h g^{-1}. This correlates to theoretical energy densities of 2,500 Wh kg^{-1} or 2,800 Wh L^{-1} based on weight or volume respectively.[3]

Two types of Li-S cells have been explored; those in which the sulfur is contained within the positive electrode host to a large degree, and those where the intermediate, highly soluble sulfur cathode redox products (shown above as S_n^{2-}) are dissolved in the electrolyte to form a "catholyte." Schematic representations of these cells are compared to a Li-ion cell in **Figure 1**. The contained cell concept benefits from higher specific energy per mass (gravimetric density) and much higher energy density per volume, owing to a lesser amount of electrolyte. Both greatly benefit from the fact that more Li^+ ions and electrons are stored in Li_2S than in an intercalation cathode, and that Li metal—with a nine-fold higher energy density than graphitic carbon—serves as the negative electrode.

Nonetheless, the exciting theoretical values are mitigated by several factors in practical translation. The inactive conducting host required to "wire up" the insulating sulfur mass also must allow for space for electrolyte ingress and volume expansion encountered on forming Li_2S at the positive electrode. Most of the cathodes and sulfur cathode composites described in the literature present an active material fraction below 60 wt% with porosity regularly above 30%. The actual volumetric density of such a positive electrode would not exceed the current level of Li-ion technologies.[13]

Other factors include larger volumes/masses of electrolyte that are necessary for typical intercalation electrodes, and the need to protect or passivate the negative electrode and utilize an excess of Li because of its inefficient cycling. Therefore, compared to Li-ion technologies, gravimetric energy density stands more to win than volumetric energy density, but both still need to be improved. Specific energies of up to 600 Wh kg^{-1} have been attained for laboratory-type contained cells, with energy densities of 150 Wh L^{-1} demonstrated for catholyte cells. The former is more than sufficient for automobile driving ranges up to 250 miles,[3] and the latter is suited to redox flow batteries for electrical grid storage.[14] However, good cycling life is a challenge, especially for cells with low electrolyte volume and high cathode loadings suited for the real-world. Scale-up to large cells also requires different cathode architecture approaches than in the world of Li-ion technologies.

The catholyte cell

The development of Li-S cells started more than half a century ago,[15–17] with relatively simple configurations that have since undergone dramatic improvements in the last half decade derived from new knowledge gained in materials and nanotechnology. Although early concepts encompassed both room- and high-temperature embodiments, problems with the high-temperature cells that utilized molten salt electrolytes started a quest for Li-S batteries operating at room temperature based on organic electrolytes, which have overtaken the field. The detailed mechanism of sulfur reduction is only beginning to be fully understood, as discussed later. Overall, reversible conversion of elemental sulfur (S_8) to lithium sulfide Li_2S takes place via highly soluble intermediate species, lithium polysulfides Li_2S_n, $3 \le n \le 8$, formed by the reduction of solid S_8 or the oxidation of solid Li_2S.[5] The term "dissolution-precipitation" is used to describe the cell chemistry, in common with Li-O_2 cells. The fact that both end products are insulators means that the conductive additives used as host materials, such as carbon, dilute the active mass and reduce both volumetric and gravimetric energy density. Most literature reports quote the capacity in terms of only sulfur mass, though, masking this contribution.

Figure 2 shows a typical voltage profile of a Li-S cell obtained at constant current. In the first discharge region centered at 2.35 V, S_8 is reduced to soluble Li_2S_n. These sulfides are poorly structurally characterized and co-exist in rapid equilibrium in solution. The second plateau at 2.1 V marks the reduction of these polysulfides to insoluble Li_2S.[18] The two regions are demarcated by a "knee" (shown in red), which represents the overpotential necessary to nucleate solid products from the supersaturated polysulfide solution. The over-potential (i.e., energy barrier, shown in blue) on the charge profile reflects the activation energy needed to oxidize the insoluble and insulating Li_2S to LiPSs (primarily

https://doi.org/10.1557/mrs.2014.86 Published online by Cambridge University Press

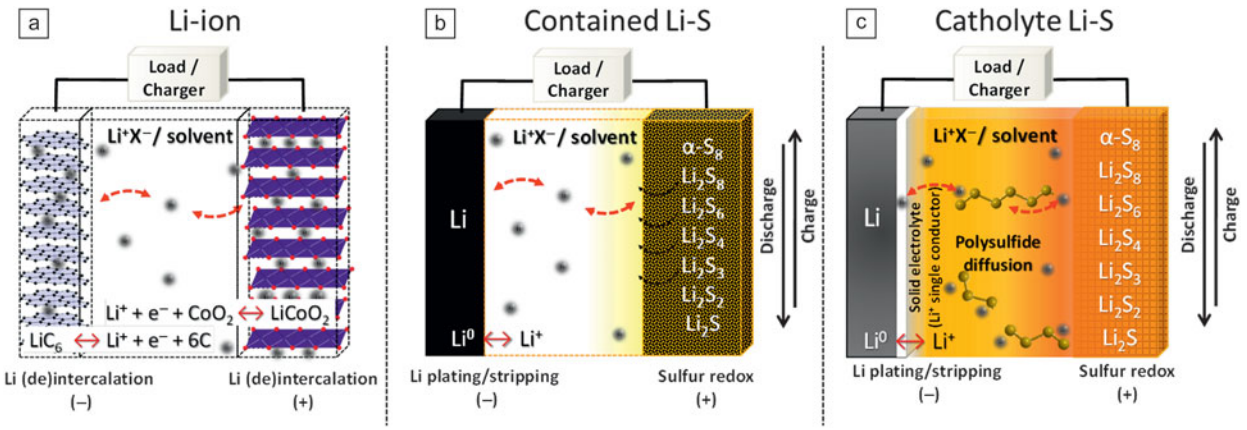


Figure 1. Schematic representation of contained Li-S and catholyte-type Li-S cells, compared to Li-ion. The (a) Li-ion battery typically comprises two intercalation materials, here graphite and lithium cobalt oxide, separated by a nonaqueous electrolyte based on a lithium salt (X– = PF_6^-, ClO_4^-, $TFSI^-$…). In contrast (b–c), Li-S batteries usually use metallic lithium as the negative electrode. In the contained Li-S architecture (b), a porous conductive host physically retains the sulfur species within the positive electrode volume, whereas the catholyte (c) functions as both the electrolyte and positive electrode. Insulation from the negative electrode is realized by a Li^+-selective membrane (represented by the white layer).

$S_4^{2-}$and S_6^{2-}). They are converted to S_8 at the last step at 2.4V.

Owing to poor cathode architecture in early Li-S cells, uncontrolled precipitation of solid products in the large pores of the cathode resulted in low capacities due to their redox inaccessibility. The development of catholyte cells, where Li_2S_n (n = 5–8) is dissolved in an organic electrolyte, was aimed at overcoming this problem.[19] The high mobility of LiPSs creates another problem, however; they readily migrate to the negative electrode, whereupon they are reduced and then diffuse back to the positive electrode and are oxidized on the next cycle. This internal "shuttle" gives rise to self-discharge and Coulombic inefficiency,[20] while providing beneficial overcharge capability.[21] The migration of active material in the electrolyte is also a cause of capacity loss during the first cycles, although recent studies suggest it does not participate in long-term capacity fading.[22,23] The main problem is the uncontrolled precipitation of Li_2S/Li_2S_2. Over cycling, insoluble agglomerates form on the surface of the positive electrode that become electrochemically inaccessible.[24,25] On the other side, the polysulfides that diffuse through the electrolyte to the Li metal surface eventually create a blocking surface of insoluble Li_2S on the negative electrode. Increased impedance and limited rechargeability result.

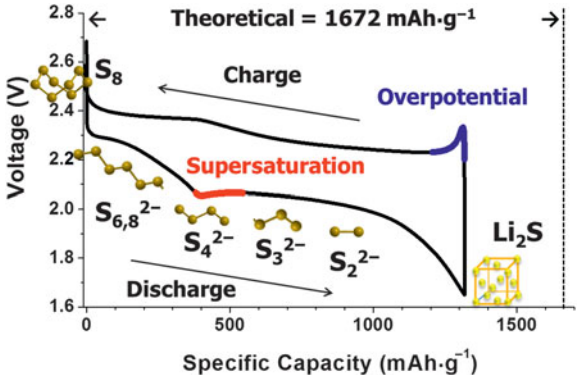


Figure 2. A typical voltage profile obtained for a Li-S battery showing the supersaturation point of lithium polysulfides in the electrolyte (red) and the overpotential (blue) encountered for the oxidation of Li_2S on charge. Structural evolution of the sulfur species upon discharge is represented, from elemental sulfur S_8 rings to chain polysulfides to solid antifluorite-type Li_2S.

These problems plagued the catholyte cell for over a decade. But recently, the concept has been revisited, partly driven by difficulties encountered with the "contained" cathode design, but also because of developments with negative electrode protection (discussed next) and in positive electrode architectures.[26,27] Applications in redox flow batteries (RFBs) have been considered, where the catholyte is designed to cycle only in the range between S_8 and Li_2S_4, avoiding problems due to the formation and volume expansion of solid Li_2S_2/Li_2S.[14] This strategy results in good cycle life and compatibility with RFB design. For a 5 M Li_2S_8 catholyte, energy densities of 97 Wh kg^{-1} and 108 Wh L^{-1} have been reported without the need for expensive ion-selective membranes (**Figure 3**).

The negative electrode

Passivation of Li metal electrodes is critical, not only to inhibit the precipitation of insoluble sulfides, but also to prevent the growth of dendrites on plating/replating of lithium. The latter creates a safety concern owing to the potential for short circuits and consumes Li via reaction of the electrolyte on each cycle by forming a continuously regenerated electrolyte interface layer. This issue has been a struggle for more than two decades,[28] although recent advances show that additives can achieve smooth, reliable dendrite-free Li

https://doi.org/10.1557/mrs.2014.86 Published online by Cambridge University Press

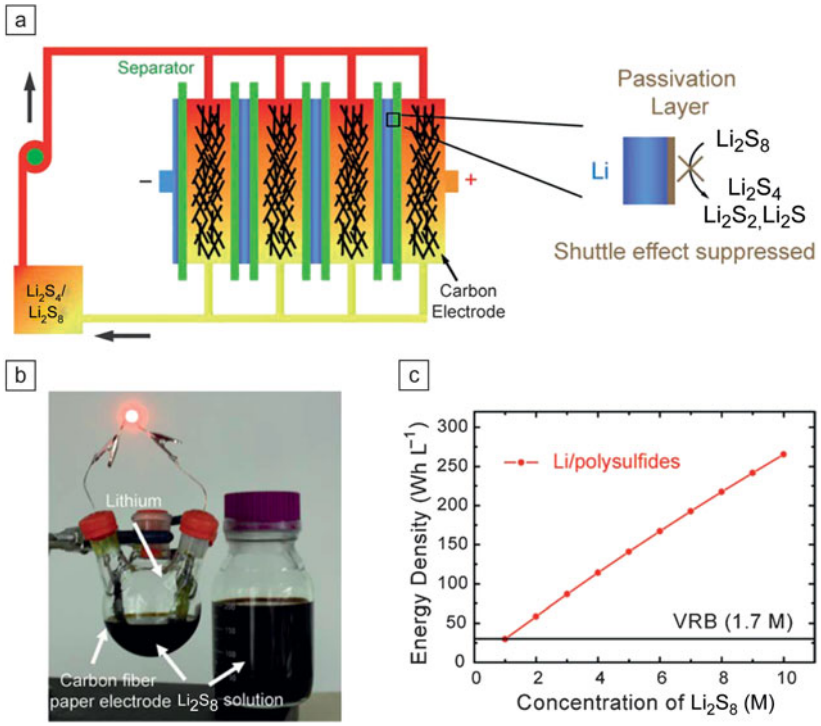


Figure 3. (a) Schematic illustrating the structure of the lithium/polysulfide (Li/PS) battery. Polysulfides flow through the system during operation and are stored in the tank in downtime. Magnified scheme on the right: the solid electrolyte interphase passivating Li due to the presence of $LiNO_3$ in the catholyte. Consequently, the shuttle effect is significantly suppressed. (b) An experimental demonstration of a membrane-free Li/PS battery with Li and the carbon fiber electrode soaked in a Li_2S_8 solution. (c) Volumetric energy density of the Li/PS system versus concentration of sulfur in the catholyte (red). The capacity of Li is set to 2000 mA h g^{-1} and 1000 mA h cm^{-3} to take the extra Li needed for practical operation into consideration. The specific capacity between sulfur and Li_2S_4 is 418 mA h g^{-1}. The black line shows the energy density of a vanadium redox flow battery (VRB) based on the vanadium catholyte and analyte only (30 W h L^{-1}). The concentrations of both catholyte and analyte are supposed to be 1.7 M, which is the commonly used stability limit for vanadium flow batteries. From this assessment, a 10-fold increase in volumetric energy density from the VRB to flow Li/PS is conceivable. Reproduced with permission from Reference 14. © 2013 Royal Society of Chemistry.

deposition.[29] This does not mitigate the LiPS shuttle and self-discharge though.

Two approaches have been explored to passivate the Li surface. One is the use of insulating protective ion-conductive membranes. Visco and coworkers at Polyplus[30] created protective membranes from lithium superionic conductors such as $Li_{(1+x+y)}Al_xTi_{(2-x)}Si_yP_{(3-y)}O_{12}$, marketed by O'Hara Glass. Owing to the titanium in the composition, they are readily reduced by Li, meaning that an interlayer between the ceramic membrane and the lithium negative electrode is necessary. This typically constitutes a thin film of a gel electrolyte.[31] A compliant seal around the assembly is also needed to accommodate the large swings in lithium volume experienced on cycling. New research in solid-state Li-ion conductors has demonstrated that lithium metal garnets are viable alternatives to phosphates. Based on the lithium-lanthanum-zirconium garnet, $Li_7La_3Zr_2O_{12}$,[32] these have the advantage of good stability to lithium metal and exhibit high conductivities when stabilized in the cubic phase.[33–35]

SION Power has developed another avenue for negative passivation by utilizing $LiNO_3$ as an electrolyte additive.[36] Work by Aurbach et al. has elucidated the mechanism behind this process, showing that it creates a protective film of Li_xNO_y and/or Li_xSO_y on the negative electrode.[37] In fact, most academic researchers exploring "contained" Li-S cell chemistry (see later) also utilize $LiNO_3$ today for this purpose, thus routinely attaining Coulombic efficiencies that approach 100%. SION Power has demonstrated the production of Li-S cells based on catholyte redox chemistry with a stabilized Li metal anode that reportedly attains a specific energy of 350 Wh/kg, but with much lower (volumetric) energy density. These have been used to store energy for solar-cell powered unmanned aerial vehicles such as the Zephyr during night-time flight.

The problem of the lithium metal electrode has also led to efforts in recent years to explore non-Li negatives. A source of Li is needed. Li_2S as a cathode has been married with a tin anode,[38] with a silicon anode,[39] and a prelithiated silicon anode in combination with a sulfur cathode.[40] However, cycle life was limited. Most recently, prelithiated silicon-carbon and hard carbon anodes in conjunction with sulfur-infused porous hollow sphere cathodes have been shown to demonstrate long cycle life of over 1000 cycles at a high capacity of 1470 mAh g^{-1}.[41]

The contained Li-S positive electrode

The alternative to the catholyte cell is to immobilize Li_2S_n in the cathode, simultaneously increasing the volumetric energy density. The porous substrate within which the Li_2S forms must be a good conductor and of low cost, hence the dominance of carbon. Because Li_2S has a lower density than elemental sulfur (1.66 g • cm^{-3} versus 2.06 g • cm^{-3}, respectively), discharge causes an 80% increase in the positive electrode volume.[42] This has to be taken into account when designing the sulfur host, because it limits the maximum sulfur content and results in severe mechanical stress and decrepitation on cycling.[43] Inventive architecture is also critical to ensure that the solid end members remain in effective contact with the host framework.

A number of porous conductive carbons with 3D-accessible nanostructures have been developed in the last five years to "contain" intermediate Li_2S_n, starting with the mesoporous carbon CMK-3.[44] It is worth noting that the degree of actual containment is often not specified, and the cells may operate partly in catholyte mode. In principle, the conductive carbon framework constrains the sulfur within the framework and

https://doi.org/10.1557/mrs.2014.86 Published online by Cambridge University Press

provides the requisite electrical contact for electron transfer to both S_8 and Li_2S at the nanoscale. Because the sulfur fraction must be adjusted to retain pathways for electrolyte/Li^+ ingress and to accommodate the active mass volume expansion during cycling, large pore volumes are required if suitably high sulfur loadings are to be attained. This can trigger dissolution of Li_2S_n without clever approaches to overcome this. Strategies to retain polysulfides at the positive electrode have utilized hydrophilic polymers to provide a chemical gradient or physical barriers to retard diffusion of the polysulfides into the electrolyte: bimodal porous carbon architectures, oxide additives and shells, and carbon interlayers. These have been recently reviewed in detail,[8–12] and a few selected advances are highlighted here.

Graphene/graphene oxide sheets are promising sulfur hosts because of their high conductivity and the wide range of compositions that can be produced through functional chemistry, utilizing the different architectures that can be constructed around sulfur particles or melt-diffused sulfur to form sandwiched/interleaved composites. Particularly important is that by controlling the ratio of reduced graphene to that of the native graphene oxide, bifunctional properties can be built in. These profit from the excellent electronic conductivity of the graphene combined with the Li_2S_n-absorption properties of the graphene oxide, while maintaining a scalable, low cost material.[45–47] The carbon host can also be coupled with a polymer coating to wrap particles and prevent any loss of active material in the electrolyte.[48] These materials also provide the opportunity to functionalize their surface with hydrophilic[44] or amphiphilic polymers.[49] This creates an even more favorable hydrophilic interaction with the soluble polysulfides and enhances contact with Li_2S, which reduces detachment of Li_2S from hydrophobic carbon surfaces. A multifaceted approach using a unique combination of surfactant-modified graphene oxide (**Figure 4**) with an elastomeric binder and an ionic liquid modified electrolyte has recently proven to be remarkably effective, achieving capacity fade rates as low as 0.039% per cycle over 1,500 cycles.[50]

Porous hollow carbon spheres (PHCSs)[51,52] and hollow carbon nanofibers[53,54] have been explored recently. PHCSs, composed of a thin porous carbon shell with a hollow interior that can be partly filled with sulfur, offer particularly high sulfur utilization and good Li_2S_n retention. Many variations have been explored following the original report by Archer et al.,[51] including synthetic approaches to thicken the carbon shell and tailor the porosity.[55] Uniformly sized 220 nm hollow porous carbon nanospheres exhibit very steady capacity behavior in typical Li-S cell configurations with a capacity retention of 99.5% over 100 cycles[56] and a much longer cycle life when coupled with a hard carbon anode.[41]

The electrolyte

An optimized electrolyte solvent or solvent blend for the Li-S system is essential to improve Li-S battery performance, but not as much effort has been expended in this regard as in cathode design. Li-ion electrolyte solvents such as alkyl carbonates react with linear chain radical polysulfides formed on cycling and cannot be used. Typical solvents are linear and cyclic ethers, such as dimethyl ether (DME) and 1,3–dioxolane,[57] with 1 M lithium bis(trifluoromethanesulfonyl)imide (LiTFSI) as the Li^+ ion carrier.[58] Although this solvent has very high LiPS solubility and good conductivity, its low boiling point makes it impractical for most commercial applications. Less volatile, more viscous electrolytes, such as ethyl methyl sulfone[44] and oligomeric polyethers (glymes),[59] have been used to improve performance.

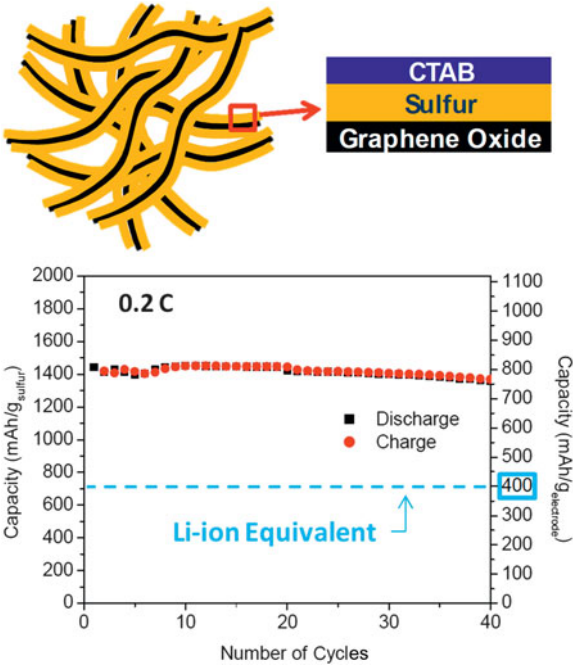


Figure 4. Schematic of the S–GO (graphene oxide) nanocomposite structure used in the multifaceted approach to Li-S cathode design. The presence of the cationic surfactant (CTAB) on the S–GO surface was shown to be critical for achieving improved cycling performance by minimizing the loss of sulfur; 1400 mAh/g_{sulfur} are delivered at a rate of C/5 (i.e., full discharge in five hours), representing a two-fold increase compared to state-of-the-art Li-ion technology (blue dashed line). Reproduced with permission from Reference 50. © 2013 American Chemical Society.

Room-temperature ionic liquids (RTILs), consisting of coordinated cations and anions, are of particular interest as electrolytes owing to their high stability, nonflammability, and nonvolatility. Recently, glyme-Li salt equimolar complexes were shown to exhibit RTIL-like behavior (e.g., non-volatility and high ionic conductivity).[60] The oxygen atoms in a glyme coordinate with Li^+ to form a complex cation, in which the Li^+ cation and the ligand (glyme) serve as the Lewis acid and Lewis base, respectively. These electrolytes showed promising results for the Li-S system, in terms of Coulombic efficiency.[61,62] This has been explained by the suppression of the redox shuttle by minimizing Li_2S_n solubility and mobility in the electrolyte, similarly to other RTILs. Amine et al. have also

https://doi.org/10.1557/mrs.2014.86 Published online by Cambridge University Press

used partially fluorinated ethers as a co-solvent with DME to greatly improve the Coulombic efficiency as well as cycling performance.[63]

During the last few years, it was shown that Li-S batteries can be cycled very well in an all–solid-state configuration.[64–66] Solid-state electrolytes have many advantages, as they diminish safety concerns and completely inhibit self-discharge. Lithium sulfide glasses such as Li_2S-P_2S_5,[67] Li_2S-SiS_2,[68] or Li_2S-GeS_2-P_2S_5[69] form the foundation of the burgeoning field of all solid-state Li-S batteries. These glasses exhibit high ionic conductivity, but hypersensitivity to air and moisture. Arsenic-substituted Li_4SnS_4 recently demonstrated improved air stability,[70] although compatibility with metallic lithium is still problematic. To alleviate this issue, the same study reported on $LiBH_4$-LiI as a chemically stable interface between sulfide solid electrolytes and Li metal.[70] On the other hand, establishing an intimate interface with the solid active cathode material can also be a challenge. Solid electrolytes and all–solid-state batteries are emerging research areas to follow and will undoubtedly impact the development of high-energy batteries.

Operando studies

Achieving full, reversible reduction from elemental sulfur down to Li_2S, beyond the typically achieved specific capacity of 1200 mAh g^{-1}, is vital to improving the energy density of Li-S batteries. However, the factors that govern capacity and cycling stability are difficult to access owing to the amorphous nature of the intermediate species and their rapid equilibration.[72,73] Fundamental studies are required to understand sulfur speciation using *in situ* probes of redox processes within a working cell. Transmission x-ray microscopy imaging carried out *operando,* for example, suggests that loss of soluble Li_2S_n outside of the electrode may not be as problematic as previously thought.[22] *Operando* X-ray diffraction studies probe solid crystalline phases, showing that Li_2S precipitation starts at the beginning of the second discharge plateau (i.e., at the super-saturation point indicated in Figure 2) and is oxidized to a different phase of elemental sulfur on charge.[74,75]

In situ electrochemical impedance spectroscopy studies, in contrast, suggest that insoluble Li_2S forms at the very end of the low-voltage plateau,[76] corresponding to the voltage drop in the profile presented in Figure 2. Barchasz et al. investigated the complex set of equilibria involved in a catholyte cell with *operando* UV spectroscopy.[72] Their studies identified S_6^{2-} and S_4^{2-} as the most probable stable polysulfides in solution and suggested that S_8^{2-} undergoes fast disproportionation via $S_8^{2-} \rightarrow S_6^{2-} + \frac{1}{4}S_8$. These findings are in accord with X-ray absorption spectroscopy (XAS) measurements carried out at the sulfur K-edge. The first *in situ* sulfur XAS study revealed the reactivity of polysulfides with alkylcarbonate solvents,[77] showing its utility as a local-probe technique.

More recently, direct monitoring of sulfur speciation over the entire redox range in real time was enabled by *operando* XAS.[55] Spectra acquired at intermediate points every 50 mAh g^{-1} in capacity were analyzed to achieve an understanding of sulfur speciation in the cell "on the fly," as summarized in **Figure 5**. One finding is that high discharge capacities (>1200 mAh/g_S) are limited by conversion of the sulfur mass at high S content. Owing to rapid disproportionation of S_8^{2-}, sulfur is formed as it is consumed on reduction. Once Li_2S nucleation is initiated at the supersaturation point, reduction proceeds rapidly through the soluble Li_2S_n, which is kinetically favored versus reaction of the residual sulfur. Such information helps explain the "nano-sized" effect that maximizes sulfur reactivity (see above), and is critical for promoting improvements in Li-S battery cathode architecture and electrolyte design.

Summary and future prospects

Practical, high energy density storage using Li-S batteries that capitalize on the low-cost features of elemental sulfur is closer to realization than ever, but fundamental challenges remain. Achieving full, reversible reduction to Li_2S is vital to increasing energy density. To accomplish this, insights into the mechanisms of sulfur redox chemistry and speciation in the cell are further needed to determine how sulfur fraction and sulfide precipitation impact capacity. The last year has seen promising reports of capacity retention of +1000 cycles. While this is predicted to continue and improve through materials discovery for both cathodes and electrolytes, a more realistic, scalable approach to materials design that aims at cells with low electrolyte volume/high electrode loading is important. Li-S presents

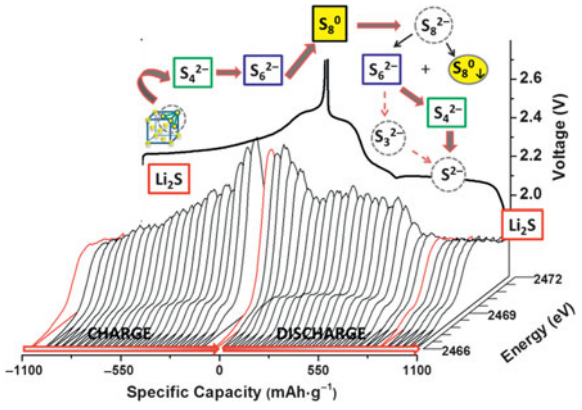


Figure 5. Schematic summarizing the overall processes proposed to occur in the Li-S cell on discharge and charge based on *operando* x-ray absorption near-edge spectroscopy. On charge, surface oxidation of Li_2S—a kinetically hindered process—leads to species such as S_4^{2-} that are consumed gradually during the sloping plateau to form Li_2S_6, with final oxidation to elemental sulfur occurring at 2.4 V. On discharge, initial reduction of elemental sulfur results in unstable S_8^{2-}, which disproportionates to S_6^{2-} and sulfur. On further electron transfer, the higher reactivity of soluble, metastable Li_2S_6 leads to a reservoir of sulfur and a cascade of intermediate polysulfides, where Li_2S_4 was identified, although the formation of S_3^{2-} and S_2^{2-} may also occur as transient species. Their rapid reduction to S^{2-} leads to supersaturation in solution, followed by delayed and sudden onset of precipitation of Li_2S at the end of the 2.1 V plateau. Reproduced with permission from Reference 55. © 2013 American Chemical Society.

https://doi.org/10.1557/mrs.2014.86 Published online by Cambridge University Press

a wealth of opportunities in this regard. Future research should also center on the development of more effective negative electrodes through solid-state ion conducting protective membranes and alternate anode materials. By surmounting these obstacles, a leap forward in energy storage could indeed be achieved.

References

1. http://www.draperprize.org/.
2. Z. Yang, J. Zhang, M.C. Kintner-Meyer, X. Lu, D. Choi, J.P. Lemmon, J. Liu, *Chem. Rev.* **111**, 3577 (2011).
3. P.G. Bruce, S.A. Freunberger, L.J. Hardwick, J.M. Tarascon, *Nat. Mater.* **11**, 19 (2012).
4. J.B. Goodenough, K.-S. Park, *J. Am. Chem. Soc.* **135**, 1167 (2013).
5. H. Yamin, E. Peled, *J. Power Sources* **9**, 281 (1983).
6. R.D. Rauh, K.M. Abraham, G.F. Pearson, J.K. Surpenant, S.B. Brummer, *J. Electrochem. Soc.* **126**, 523 (1979).
7. X. Ji, L.F. Nazar, *J. Mater. Chem.* **20**, 9821 (2010).
8. S. Evers, L.F. Nazar, *Acc. Chem. Res.* **46**, 1135 (2013).
9. A. Manthiram, Y. Fu, Y.-S. Su, *Acc. Chem. Res.* **46**, 1125 (2013).
10. Y.X. Yin, S. Xin, Y.G. Guo, L.J. Wan, *Angew. Chem. Int. Ed.* **52**, 13186 (2013).
11. Y. Yang, G. Zheng, Y. Cui, *Chem. Soc. Rev.* **42**, 3018 (2013).
12. D.-W. Wang, Q. Zeng, G. Zhou, L. Yin, F. Li, H.-M. Cheng, I.R. Gentle, G.Q.M. Lu, *J. Mater. Chem. A* **1**, 9382 (2013).
13. M. Hagen, S. Dörfler, P. Fanz, T. Berger, R. Speck, J. Tübke, H. Althues, M.J. Hoffmann, C. Scherr, S. Kaskel, *J. Power Sources* **224**, 260 (2013).
14. Y. Yang, G. Zheng, Y. Cui, *Energy Environ. Sci.* **6**, 1552 (2013).
15. D. Herbert, D.J. Ulam, US Patent 3043896 (1962).
16. M.L.B. Rao, US Patent 3,413,154 (1968).
17. D. Nole, V. Moss, US Patent 3532543 (1970).
18. J.R. Akridge, Y.V. Mikhaylik, N. White, *Solid State Ionics* **175**, 243 (2004).
19. R.D. Rauh, F.S. Shuker, J.M. Marston, S.B. Brummer, *J. Inorg. Nucl. Chem.* **39**, 1761 (1977).
20. H.S. Ryu, H.J. Ahn, K.W. Kim, J.H. Ahn, J.Y. Lee, E.J. Cairns, *J. Power Sources* **140**, 365 (2005).
21. B.M.L. Rao, J.A. Shropshire, *J. Electrochem. Soc.* **128**, 942 (1981).
22. J. Nelson, S. Misra, Y. Yang, A. Jackson, Y. Liu, H. Wang, H. Dai, H. Andrews, Y. Cui, M.F. Toney, *J. Am. Chem. Soc.* **134**, 6337 (2012).
23. Y. Diao, K. Xie, S. Xiong, X.J. Hong, *J. Electrochem. Soc.* **159**, A421 (2012).
24. C. Barchasz, J.-C. Lepêtre, F. Alloin, S. Patoux, *J. Power Sources* **199**, 322 (2011).
25. S.E. Cheon, K.S. Ko, J.H. Cho, S.W. Kim, E.Y. Chin, H.T. Kim, *J. Electrochem. Soc.* **150**, A796 (2003).
26. R. Demir-Cakan, M. Morcrette, A.G. Gangulibabu, R. Dedryvère, J.-M. Tarascon, *Energy Environ. Sci.* **6**, 176 (2013).
27. Y. Fu, Y.S. Su, A. Manthiram, *Angew. Chem. Int. Ed.* **52**, 6930 (2013).
28. K.M. Abraham, S.B. Brummer, in *Lithium Batteries*, J.P. Gabano, Ed. (Academic Press, London, 1983), chap. 14.
29. F. Ding, W. Xu, G.L. Graff, J. Zhang, M.L. Sushko, X. Chen, Y. Shao, M.H. Engelhard, Z. Nie, J. Xiao, X. Li, P.V. Sushko, J. Liu, J.-G. Zhang, *J. Am. Chem. Soc.* **135**, 4450 (2013).
30. S.J. Visco, M.Y. Chu, US Patent 6,210,832 (2001).
31. T. Zhang, N. Imanishi, Y. Shimonishi, A. Hirano, J. Xie, Y. Takeda, O. Yamamoto, N. Sammes, *J. Electrochem. Soc.* **157**, A214 (2010).
32. R. Murugan, V. Thangadurai, W. Weppner, *Angew. Chem. Int. Ed.* **46**, 7778 (2007).
33. P. Knauth, *Solid State Ionics* **180**, 911 (2009).
34. S. Ohta, T. Kobayashi, T. Asaoka, *J. Power Sources* **196**, 3342 (2011).
35. E. Shinawi, J. Janek, *J. Power Sources* **225**, 13 (2013).
36. Y.V. Mikhaylik, US Patent 7,352,680 (2008).
37. D. Aurbach, E. Pollak, R. Elazari, G. Salitra, C.S. Kelley, J. Affinito, *J. Electrochem. Soc.* **156**, A694 (2009).
38. J. Hassoun, B. Scrosati, *Angew. Chem. Int. Ed.* **49**, 2371 (2010).
39. Y. Yang, M.T. McDowell, A. Jackson, J.J. Cha, S.S. Hong, Y. Cui, *Nano Lett.* **10**, 1486 (2010).
40. R. Elazari, G. Salitra, G. Gershinsky, A. Garsuch, A. Panchenko, D. Aurbach, *Electrochem. Commun.* **14**, 21 (2012).
41. J. Brückner, S. Thieme, F. Böttger-Hiller, I. Bauer, H.T. Grossmann, P. Strubel, H. Althues, S. Spange, S. Kaskel, *Adv. Funct. Mater.* **24** (9), 1284 (2013).
42. X. He, J. Ren, L. Wang, W. Pu, C. Jiang, C. Wan, *J. Power Sources* **190**, 154 (2009).
43. R. Elazari, G. Salitra, Y. Talyosed, J. Grinblat, C. Scordilis-Kelley, A. Xiao, J. Affinito, D. Aurbach, *J. Electrochem. Soc.* **157**, A1131 (2010).
44. X. Ji, K. T. Lee, L.F. Nazar, *Nat. Mater.* **8**, 500 (2009).
45. L. Ji, M. Rao, H. Zheng, L. Zhang, Y. Li, W. Duan, J. Guo, E.J. Cairns, Y. Zhang, *J. Am. Chem. Soc.* **133**, 18522 (2011).
46. S. Lu, Y. Cheng, X. Wu, J. Liu, *Nano Lett.* **13**, 2485 (2013).
47. R.J. Chen, T. Zhao, J. Lu, F. Wu, L. Li, J.Z. Chen, G.Q. Tan, Y.S. Ye, K. Amine, *Nano Lett.* **13**, 4642 (2013).
48. H. Wang, Y. Yang, Y. Liang, J.T. Robinson, Y. Li, A. Jackson, Y. Cui, H. Dai, *Nano Lett.* **11**, 2644 (2011).
49. G. Zheng, Q. Zhang, J.J. Cha, Y. Yang, W. Li, Z.W. Seh, Y. Cui, *Nano Lett.* **13**, 1265 (2013).
50. M.K. Song, Y. Zhang, E.J. Cairns, *Nano Lett.* **13**, 5891 (2013).
51. N. Jayaprakash, J. Shen, S.S. Moganty, A. Corona, L.A. Archer, *Angew. Chem. Int. Ed.* **123**, 6026 (2011).
52. J. Kim, D.J. Lee, H.-G. Jung, Y.-K. Sun, J. Hassoun, B. Scrosati, *Adv. Funct. Mater.* **23**, 1076 (2013).
53. J. Guo, Y. Xu, C. Wang, *Nano Lett.* **11**, 4288 (2011).
54. G. Zheng, Y. Yang, J.J. Chan, S.S. Hong, Y. Cui, *Nano Lett.* **11**, 4462 (2011).
55. M. Cuisinier, P.-E. Cabelguen, S. Evers, G. He, M. Kolbeck, A. Garsuch, T. Bolin, M. Balasubramanian, L.F. Nazar, *J. Phys. Chem. Lett.* **4**, 3227 (2013).
56. G. He, S. Evers, X. Liang, M. Cuisinier, A. Garsuch, L.F. Nazar, *ACS Nano* **7**, 10920 (2013).
57. E. Peled, A. Gorenshtein, M. Segal, Y. Sternberg, *J. Power Sources* **26**, 269 (1989).
58. H.S. Kim, C.-S. Jeong, *Bull. Korean Chem. Soc.*, **32**, 3682 (2011).
59. L.X. Yuan, J.K. Feng, X.P. Ai, Y.L. Cao, S.L. Chen, H.X. Yang, *Electrochem. Commun.* **8**, 610 (2006).
60. T. Tamura, T. Hachida, K. Yoshida, N. Tachikawa, K. Dokko, M. Watanabe, *J. Power Sources* **195**, 6095 (2010).
61. J.-W. Park, K. Yamauchi, E. Takashima, N. Tachikawa, K. Ueno, K. Dokko, M. Watanabe, *J. Phys. Chem. C* **117**, 4431 (2013).
62. L. Suo, Y.S. Hu, H. Li, M. Armand, L. Chen, *Nat. Commun.* **4**, 1481 (2013).
63. W. Weng, V.G. Pol, K. Amine, *Adv. Mater.* **25**, 1608 (2013).
64. A. Sakuda, A. Hayashi, M. Tatsumisago, *Sci. Rep.* **3**, 2261 (2013).
65. M. Agostini, Y. Aihara, T. Yamada, B. Scrosati, J. Hassoun, *Solid State Ionics* **244**, 48 (2013).
66. Z. Lin, Z.C. Liu, N.J. Dudney, C.D. Liang, *ACS Nano* **7**, 2829 (2013).
67. M. Nagao, A. Hayashi, M. Tatsumisago, *Electrochim. Acta* **56**, 6055 (2011).
68. N. Machida, K. Kobayashi, Y. Nishikawa, T. Shigematsu, *Solid State Ionics* **175**, 247 (2004).
69. T. Kobayashi, Y. Imade, D. Shishihara, K. Homma, M. Nagao, R. Watanabe, T. Yokoi, A. Yamada, R. Kanno, T. Tatsumi, *J. Power Sources* **182**, 621 (2008).
70. G. Sahu, Z. Lin, J. Li, Z. Liu, N. Dudney, C. Liang, *Energy Environ. Sci.* **7**, 1053 (2014).
71. T. Takeuchia, H. Kageyama, K. Nakanishi, T. Ohta, A. Sakuda, H. Sakaebe, H. Kobayashi, K. Tatsumi, Z. Ogumi, *Electrochem. Lett.* **3**, A31 (2014).
72. C. Barchasz, F. Molton, C. Duboc, J.C. Leprêtre, S. Patoux, F. Alloin, *Anal. Chem.* **84**, 3973 (2012).
73. M.U.M. Patel, R. Demir-Cakan, M. Morcrette, J.-M. Tarascon, M. Gaberscek, R. Dominko, *ChemSusChem* **6** (7), 1177 (2013).
74. S. Walus, C. Barchasz, J.F. Colin, J.F. Martin, E. Elkaim, J.C. Lepretre, F. Alloin, *Chem. Commun.* **49**, 7899 (2013).
75. C. Villevieille, P. Novak, *J. Mater. Chem. A* **1**, 13089 (2013).
76. L. Yuan, X. Qiu, L. Chen, W. Zhu, *J. Power Sources* **189**, 127 (2009).
77. J. Gao, M.A. Lowe, Y. Kiya, H.D. Abruña, *J. Phys. Chem. C* **115**, 25132 (2011). □



https://doi.org/10.1557/mrs.2014.86 Published online by Cambridge University Press